ChemPubSoc Europe

DOI: 10.1002/open.201500210

Open Access ChemistryOPEN Full Papers

Extending the Study of the 6,8 Rearrangement in Flavylium Compounds to Higher pH Values: Interconversion between 6-Bromo and 8-Bromo-apigeninidin

Luís M. Cruz[+],[a] Nuno M. Basílio[+],[b] Victor A. de Freitas,*[a] João C. Lima,[b] and Fernando J. Pina*[b]

The rearrangement between isomers 6- and 8-bromo-apigeninidin (**6** and **8**) was studied by pH jumps using stopped flow, UV/Vis, NMR, and HPLC analysis. The system constitutes a pH-dependent network of chemical reactions involving up to 18 different species. The dynamic network is equivalent to a single diprotic acid exhibiting two pK_as, 2.55 and 5.4. Similar to other flavylium derivatives, the mole fraction of the species hemiketal and *cis*-chalcone in both multistate isomers are negligible at the equilibrium. At pH 1, the pure isomers are slowly converted in a mixture containing about 50% of isomers **6** and **8**, while at pH 4, the system evolves to mixture of 10% *trans*-chalcone and 90% of quinoidal bases. A series of pH jumps from pure isomer **6** at pH 1 to pH 6 and back to pH 1 leads to the same initial absorption spectra of the pure isomer **6**. The same occurs for pure isomer **8**, showing the lack of communication between the *cis*-chalcones, at least in the time scale of few minutes. A pH jump from the equilibrated mixture of the isomers at pH 1.0 to 5.8 permits to follow a very slow isomerization.

Introduction

3-Deoxyanthocyanidins form a family of flavylium derivatives appearing in ferns and mosses, as well as hybrids of sorghum and purple corn.[1–7] Like anthocyanins, they are involved in a multistate system as shown in Scheme 1 for apigeninidin.

Both hydration and proton transfer equilibria are dependent on the proton concentration, Scheme 1, and by consequence, addition of acid is expected to shift the multiequilibrium towards flavylium cation, which is the sole species at sufficiently acidic solutions.

In spite of the complexity of the multiequilibrium, the system can be simplified considering a single acid base reaction involving the species $\mathbf{AH^+}$ and its conjugate base **CB**, defined as the sum of the other species: **A**, **B**, **Cc**, and **Ct**, [Equation (1)].

$$\mathbf{AH^+} + H_2O \rightleftharpoons \mathbf{CB} + H_3O^+ \quad K'_a = K_a + K_h + K_hK_t + K_hK_tK_i \qquad (1)$$

With $[\mathbf{CB}] = [\mathbf{A}] + [\mathbf{B}] + [\mathbf{Cc}] + [\mathbf{Ct}]$

The mole fraction distribution of the conjugate base, **CB**, is dramatically dependent on the substitution pattern of the 2-phenylbenzopyrylium core. In the case of apigeninidin, Scheme 1, the mole fraction distribution of the five species in acidic medium can be calculated from data previously reported (Figure 1).[8–9]

A very useful procedure to study the flavylium multistates is the use of pH jumps. A direct pH jump is here defined as addition of base to an equilibrated solution of the compound at pH 1 ($\mathbf{AH^+}$), while a reverse pH jump as the addition of acid to an equilibrated solution at higher pH values, for example pH 6, back to lower pH values (in particular, pH 1). The stopped flow technique should be used when the respective rates occur in the order of seconds to subseconds.

The faster reaction after a direct pH jump is by far proton transfer, [Eq. (2)] (not observed by stopped flow). Quinoidal base A is thus formed during the mixing time of the base.

$$\mathbf{AH^+} + H_2O \rightleftharpoons \mathbf{A} + H_3O^+ \qquad K_a \qquad (2)$$

[a] *L. M. Cruz,[+] V. A. de Freitas*
Laboratório Associado para a Química Verde (LAQV)
Rede de Química e Tecnologia (REQUIMTE)
Departamento de Química e Bioquímica
Faculdade de Ciências, Universidade do Porto
Rua do Campo Alegre, 687, 4169-007 Porto (Portugal)
E-mail: vfreitas@fc.up.pt

[b] *N. M. Basílio,[+] J. C. Lima, F. J. Pina*
Laboratório Associado para a Química Verde (LAQV)
Rede de Química e Tecnologia (REQUIMTE)
Departamento de Química, Faculdade de Ciências e Tecnologia
Universidade Nova de Lisboa, 2829-516 Caparica (Portugal)
E-mail: fp@fct.unl.pt

[+] *These two authors contributed equally to this work.*

Supporting information and the ORCID identification numbers for the authors of this article can be found under http://dx.doi.org/10.1002/open.201500210.

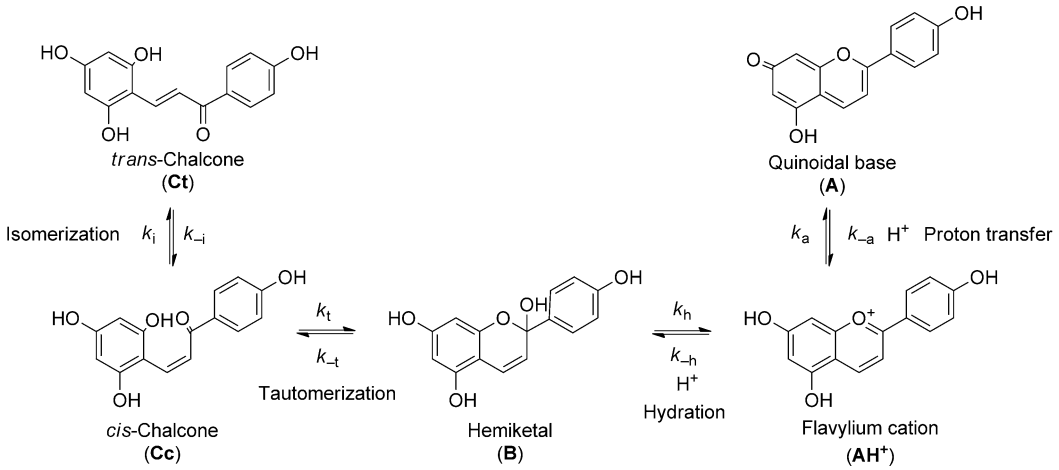

Scheme 1. Multistate system of apigeninidin.

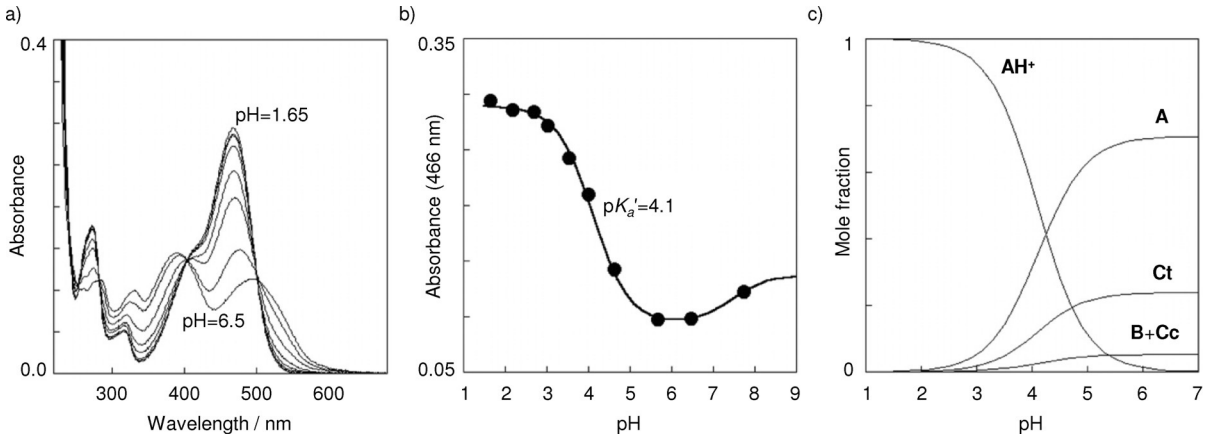

Figure 1. a) Absorption spectra of equilibrated solutions of apigeninidin as a function of pH. b) Absorbance registered at 466 nm as a function of pH. This data was fitted with a $pK'_a = 4.1$ and a second pK''_a around 7 was observed at higher pH values. c) Mole fraction distribution of apigeninidin in acidic medium.

A slower process that is pH dependent and can be monitored by stopped flow or through a common spectrophotometer is the hydration forming **B** that competes with **A** for the $\mathbf{AH^+}$ disappearance, [Eq. (3)].

$$\mathbf{AH^+} + 2\,H_2O \rightleftharpoons \mathbf{B} + H_3O^+ \qquad K_h \tag{3}$$

The hydration is followed by the tautomerization (ring opening/closure) which is faster than hydration unless the pH is very low, [Eq. (4)].

$$\mathbf{B} \rightleftharpoons \mathbf{Cc}\ K_t \tag{4}$$

A and $\mathbf{AH^+}$ are in a very fast equilibrium; **B** and **Cc** are also in a fast equilibrium, while much slower (subseconds). Both of these equilibria ($\mathbf{AH^+}$/**A** and **B**/**Cc**) are faster than hydration unless at very acidic pH values, where hydration could be faster than tautomerization due to its direct dependence on $[H^+]$. One important breakthrough on this system was reported by Brouillard and Dubois (1977),[10] in which the quinoidal base does not react in moderately acidic medium and, by consequence, the system evolves towards the other species through the hydration reaction of the flavylium cation. The system equilibrates to give **Ct** through the isomerization, which could be very slow or take place in subseconds, depending on the value of the *cis–trans* isomerization barrier. The mathematical expressions to account for the kinetics of the direct pH jumps are different in both cases and have been reported previously.[11]

One interesting feature to explore in deoxyanthocyanidins is the possibility of two different pathways for the *cis*-chalcone ring closure to give the hemiketal followed by formation of flavylium cation, Scheme 2.[12–13] If the substituents in position 6 and 8 of the flavylium cation are equal, the two pathways lead to the same isomer. However, if they are different, two distinguishable isomers are obtained. The first description of the 6,8 rearrangement was reported by Jurd for the compound 4′,6,7,8 tetrahydroxyflavylium, Scheme 2.[13] He observed that at pH 2.6, the isomer bearing a hydroxy group in position 6 gives, almost quantitatively, the one in position 8 after about seven hours, while in 1% aqueous hydrochloric acid at room temperature, this was much slower (~ three days). More recently, An-

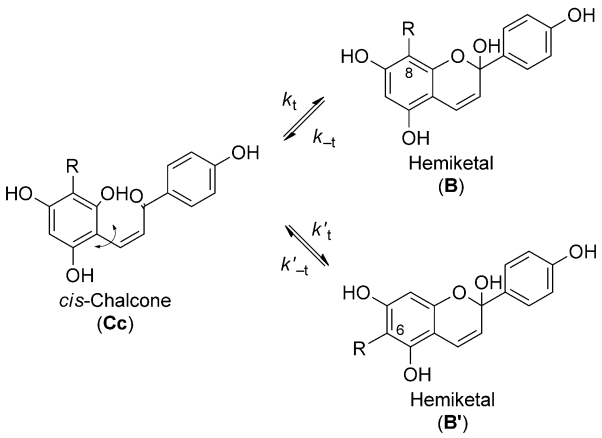

Scheme 2. Illustrating the two possibilities of ring opening–closure in flavylium compounds with different substitution patterns in position 6 and 8, according to Jurd.[13]

derson and co-workers[12] reported a complete study of flavylium cations isomerization derived from the *C*-glycosyl-3-deoxyanthocyanidin family and arrived at similar conclusions.

The scope of this work is to extend the 6,8 rearrangement to less acidic medium in order to access the other species of the multistate. The questions are: 1) How distributed are the quinoidal base isomers 6- and 8-bromo-apigeninidin (**6** and **8**, respectively), hemiketal, *cis*- and *trans*-chalcones, and the respective ionized species in a large pH range? 2) How are the kinetics of multistates of isomers **6** and **8** related?

Results and Discussion

Synthesis

Compounds **6** and **8** were synthesized according the reactions described in Scheme 3.

Bromination of 2,4,6-trihydroxyaldehyde (**1**) was performed in tetrahydrofuran (THF) at −20 °C using pyridinium tribromide giving the product **2** with 89% yield. Acidic aldol condensation between compound **2** and 4-hydroxyacetophenone (**3**) in acetic acid at room temperature gave a mixture of isomers **6** and **8**. These compounds were further purified and isolated from impurities by semipreparative high-performance liquid chromatography (HPLC) and analyzed by liquid chromatography with diode array detection paired with electrospray ionization mass spectrometry (LC-DAD/ESI-MS) in positive-ion mode giving a molecular ion, $[M]^+$ at *m/z* 333, 335. This agrees with the flavylium cation mass and is typical for compounds possessing a bromide atom in their structure ($^{79}Br/^{81}Br$) (Figure 2). The structure of the two isomers were fully confirmed by ^1H and ^{13}C NMR assignment using 1D and 2D NMR techniques (correlation spectroscopy, COSY; heteronuclear single quantum coherence spectroscopy, HSQC; and heteronuclear multiple bond correlation spectroscopy, HMBC) in CD_3OD/CF_3COOH 90:10 (see Experimental Section).

The electronic transitions of the isomers were calculated with AM1-CI[14] (99 single excited configurations interaction) after geometry optimization (MM+), without correction for the solvent. The results for the two lowest singlet transition energies of apigeninidin, 6-bromo-apigeninidin, and 8-bromo-apigeninidin are summarized in Table 1.

Table 1. Calculated wavelengths (λ) and oscillator strengths (F) for the two lowest transitions of apigenidin, 6-bromo-apigenidin, and 8-bromo-apigenidin.

Compound	S0→S1		S0→S2		Peak separation [nm]
	λ [nm]	*F*	λ [nm]	*F*	
Apigeninidin	381	0.922	326	0.125	55
Isomer **6**	389	0.790	364	0.081	25
Isomer **8**	379	0.906	329	0.160	50

At this simple level of calculation and without taking in consideration solvation effects, the absolute values for the transitions cannot be taken quantitatively; however, valuable qualitative information can be obtained. Bromo substitution in position 6 leads to a significant red shift of the S0→S2 transition to energies close to the S0→S1 transition, while bromo substitution in position 8 does not change significantly the transitions with respect to the parent apigenidin. Thus,

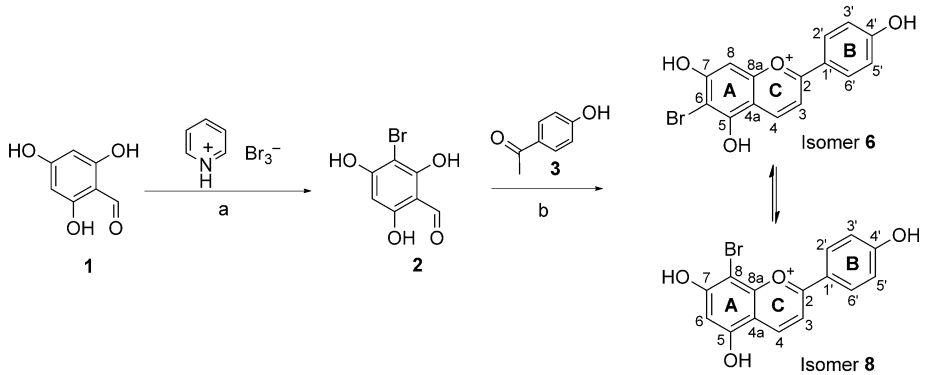

Scheme 3. Synthetic strategy to obtain flavylium compounds (isomers **6** and **8**). *Reagents and conditions*: a) THF, −20 °C, 3 h, 89%; b) HCl (g) (60 min), HOAc, rt, 24 h, 6%.

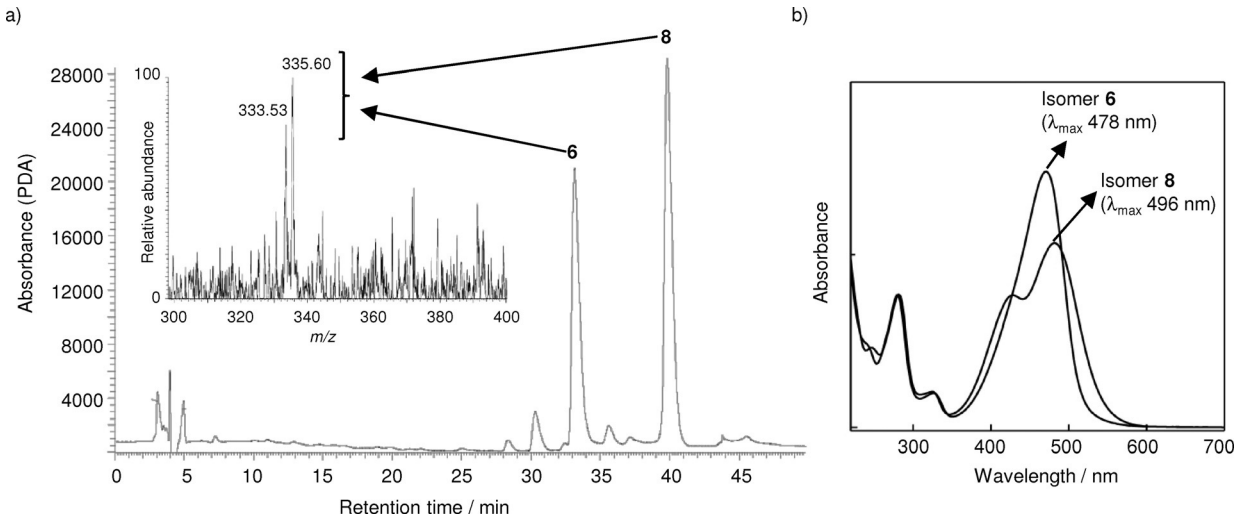

Figure 2. a) LC-PDA chromatogram of isomers **6** and **8**. Inset: Full MS spectrum of isomers **6** and **8**. b) UV/Vis spectra of isomers **6** and **8**.

while the 8-bromo substituted is predicted to display two lower energy transitions separated by about 50 nm, in the 6-bromo-substituted isomer, the separation is only 25 nm, and the S0→S2 transition is merged with the S0→S1 transition. This attribution is also in accordance to the absorption spectra reported by Anderson for the *C*-glycosyl-3-deoxyanthocyanidins.[12]

Equilibria

The multistate of chemical reactions expected for the system are presented in Scheme 4.

Before going through the results, it is relevant to stress that from a theoretical point of view, the two multistate equilibria involving the isomer **6** (multistate 6) and isomer **8** (multistate 8) are only able to communicate through the *cis*-chalcones and *trans*-chalcones. Anticipating the ^{1}H NMR results at the equilibrium, no *cis*-chalcone or hemiketal were observed, and only a set of signals attributed to a single *trans*-chalcone species was detected.

The analytical expressions for the mole fraction distribution of the network species reported in Scheme 4, at the equilibrium, are deduced in Appendix 1 in the Supporting Information. The network behaves as a single acid–base equilibrium involving the two flavylium cation isomers and the respective conjugated bases, [Eq. (5)] and [Eq. (6)], with an apparent acidity constant given by [Eq. (7)]. Note: subscripts in these equations do not refer to multiple species; rather, simply the isomer type.

$$\mathbf{AH^+}_6 + \mathbf{AH^+}_8 + H_2O \rightleftharpoons \mathbf{CB}_6 + \mathbf{CB}_8 + H_3O \qquad K'_{ap} \tag{5}$$

$$\text{With } [\mathbf{CB}_6] = [\mathbf{A}_6] + [\mathbf{B}_6] + [\mathbf{Cc}_6] + [\mathbf{Ct}_6] \text{ and } [\mathbf{CB}_8] = [\mathbf{A}_8] + [\mathbf{B}_8] + [\mathbf{Cc}_8] + [\mathbf{Ct}_8] \tag{6}$$

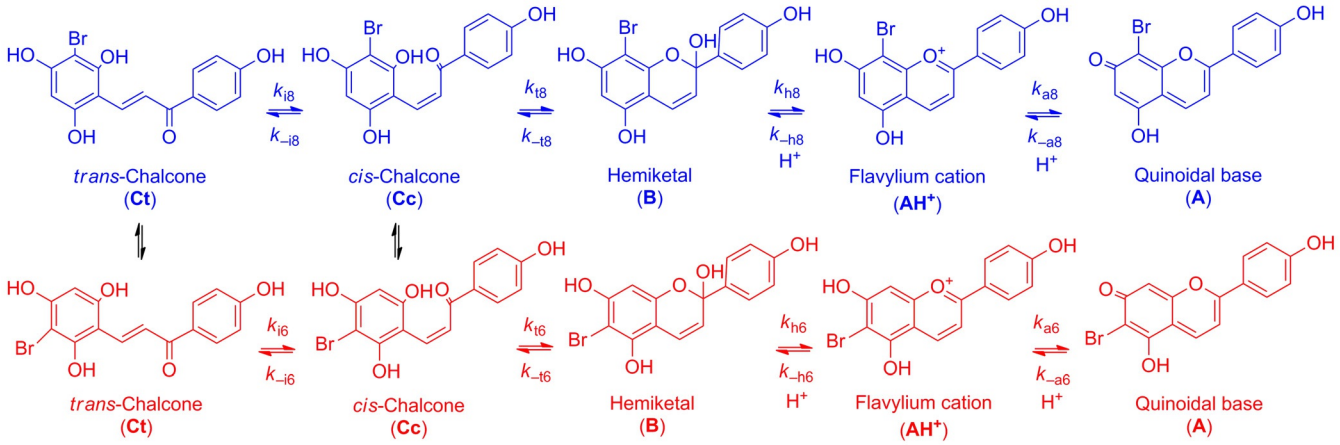

Scheme 4. Multistate system of bromo-apigeninidin isomers (**6** and **8**) up to pH 4. The two systems could, in principle, communicate through the chalcones' equilibria.

$$K'_{ap} = \frac{K_{AH^+,6,8}(K_{a6} + K_{h6} + K_{h6}K_{t6} + K_{h6}K_{t6}K_{i6}) + K_{a8} + K_{h8} + K_{h8}K_{t8} + K_{h8}K_{t8}K_{i8}}{(1 + K_{AH^+,6,8})}$$

$$= \frac{K_{AH^+,6,8}K'_{a6} + K'_{a8}}{(1 + K_{AH^+,6,8})} \quad (7)$$

with the ratio between the two flavylium cation isomers defined by [Eq. (8)], and the remaining constants as reported in Scheme 3.

$$K_{AH^+6,8} = \frac{[\mathbf{AH_6^+}]}{[\mathbf{AH_8^+}]} \quad (8)$$

As shown in appendix 1, the mole fraction distribution of the sum of the two flavylium cation isomers and the respective conjugated bases is given by [Eq. (9)].

$$X_{\mathbf{AH_6^+}+\mathbf{AH_8^+}} = \frac{[\mathbf{AH_6^+}] + [\mathbf{AH_8^+}]}{\mathbf{C_0}} = \frac{[H^+]}{[H^+] + K'_{ap}}$$
$$X_{\mathbf{CB_6}+\mathbf{CB_8}} = \frac{[\mathbf{CB_6}] + [\mathbf{CB_8}]}{\mathbf{C_0}} = \frac{K'_{ap}}{[H^+] + K'_{ap}} \quad (9)$$

Isomer conversion at pH 1.0

According to the ^{1}H NMR data, the equilibrated solutions of the compound at pH 1.0 are mixtures of the two isomers. This mixture was separated by HPLC, and both isomers were lyophilized. The spectral evolution of pure isomer **6** after dissolution in a mixture ethanol:water (1:4) is reported in Figure 3a.

The absorption spectrum of isomer **6** decreases due to its partial conversion into isomer **8** until the equilibrium mixture is reached at this pH and temperature. On the other hand, the absorption spectrum increases around 525 and 350 nm owing to the formation of isomer **8**, which has a higher extinction coefficient in this spectral region. This behavior is similar to previous results reported by Jurd[13] and Anderson[12] (Figure 2a). In Figure 2b, the absorption spectra of both isomers, as well as the equilibrium, are shown. Spectral decomposition of the equilibrium absorption leads to 52% isomer **8** and 48% isomer **6**, $K_{AH+6,8} = 1.1 \pm 0.1$

NMR

In order to study the equilibria network of the two isomers, ^{1}H NMR experiments with pD variation were performed in D_2O:EtOD 80:20 ($C = 0.2$ mM) (Figure 4). It can be observed that rapid proton transfer reactions of the flavylium cations of the two isomers occurred as pH increases, giving the respective bases. This was visualized by the chemical shift displacement of the H–4C of the pair **AH$^+$**/**A** to higher fields. A small amount of a single *trans*-chalcone (**Ct**) for higher pD values was also observed. On the other hand, at equilibrium, the presence of hemiketal (**B**) and *cis*-chalcone (**Cc**) species was not observed. Through the behavior of the signals attributed to H–4C and H–3C, it was also observed that the equilibrium shifts towards a higher proportion of the isomer **6** relative to isomer **8** as long as the pH increases.

HPLC

Chromatographic experiments were also performed in order to confirm the displacement of the isomers' equilibrium with the pH (Figure 5). It was observed that at pH 1, isomer **8** slightly predominates over isomer **6**. However, as long as pH increases to moderate acidic and neutral solutions, the proportion changes, and isomer **6** becomes more abundant at the equilibrium. These results are in agreement with the NMR and UV/Vis data.

Equilibrium

The pH-dependent UV/Vis spectral variations of equilibrated solutions of the two isomers are reported in Figure 6. Due to the existence of several hydroxy substituents in the structure, the quinoidal bases, hemiketal, and both chalcones can deprotonate. In acidic medium, two global acid–base equilibria

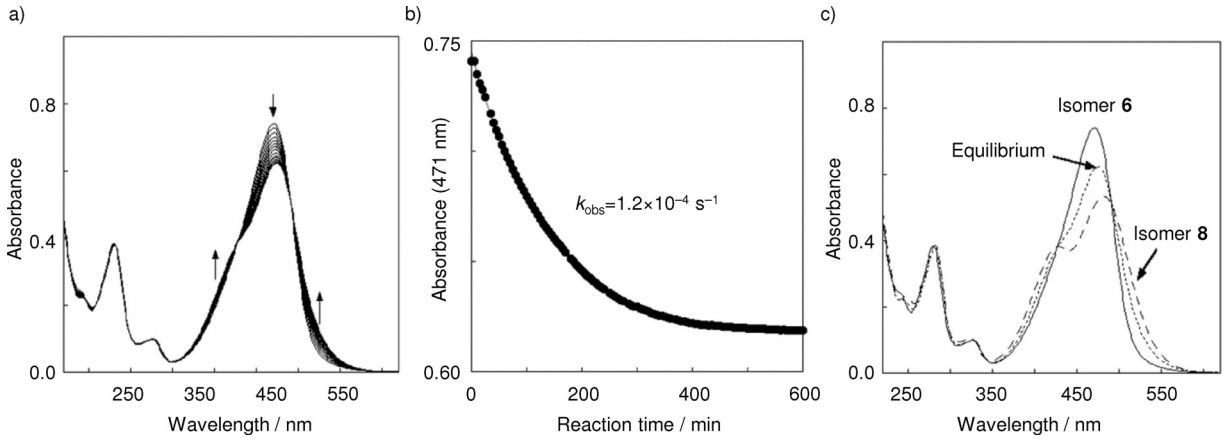

Figure 3. a) Spectral variations of isomer **6** (7×10^{-5} M) upon separation by HPLC; pH 1.0; in water:EtOH (4:1, *v:v*). b) Absorbance variations at 471 nm as a function of time showing pseudo-first-order kinetics fitted with $k_{obs} = 1.2 \times 10^{-4}$ s^{-1}. c) Absorption spectra of both isomers (7×10^{-5} M). The equilibrium is a mixture of 52% isomer **8** and 48% isomer **6**, obtained by spectral decomposition.

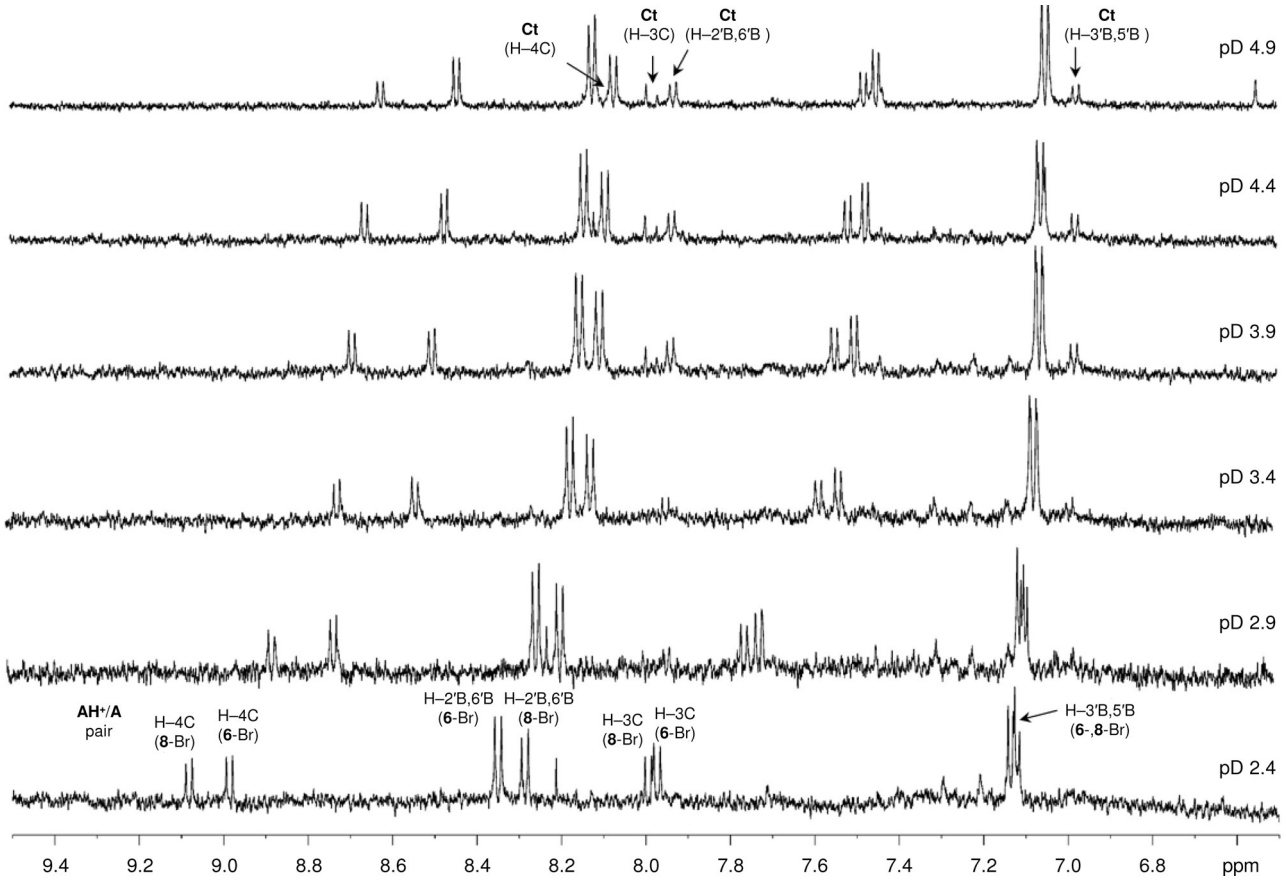

Figure 4. ^{1}H NMR spectra experiments with pD variation (D_2O:EtOD 80:20) at 0.2 mM (each pD solution was left to equilibrate for 2 h before the spectrum was taken).

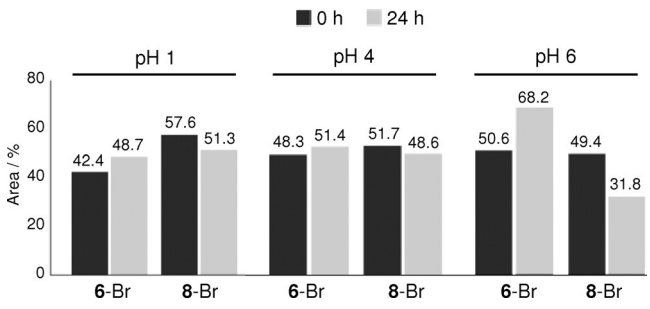

Figure 5. Variation of isomer proportion with pH and with time in solutions of H_2O/EtOH 80:20 at 0.27 mM.

are observed. The system can be accounted for by [Eq. (10)] and [Eq. (11)].

$$\mathbf{AH}^{+} + H_2O \rightleftharpoons \mathbf{CB} + H_3O^{+} \qquad K'_a \qquad (10)$$

$$\mathbf{CB} + H_2O \rightleftharpoons \mathbf{CB}^{-} + H_3O^{+} \qquad K''_a \qquad (11)$$

where [**CB**] is now defined as the sum of the species [$\mathbf{A_6}$] + [$\mathbf{A_8}$] + [$\mathbf{B_6}$] + [$\mathbf{B_8}$] + [$\mathbf{Cc_6}$] + [$\mathbf{Cc_8}$] + [$\mathbf{Ct_6}$] + [$\mathbf{Ct_8}$], and [$\mathbf{CB}^{-}$] is the identical sum for monoionized species.

According to Figure 6, the equilibrium between $\mathbf{AH}^{+}$ and **CB** shows a $pK'_a = 2.55$, and the second one between **CB** and $\mathbf{CB}^{-}$ $pK''_a = 5.4$. Inspection of Figure 6a,b indicates that **CB** and $\mathbf{CB}^{-}$, should be mainly constituted by quinoidal bases, due to the shape and position of the respective absorption spectra. Further information is obtained by following the kinetic processes to reach the equilibrium upon a direct pH jump. Figure 7a shows that a direct pH jump from the equilibrated solution of the two isomers at pH 1.0 to 3.4 was followed by stopped flow. Practically no absorption changes take place at this pH value and time scale, showing that the quinoidal bases are not consumed after one second, and the ratio between $\mathbf{A_8}$ and $\mathbf{A_6}$ is similar to that observed for the flavylium cations at pH = 1.

On the other hand, an identical direct pH jump to 3.5 followed in a longer timescale showed the existence of a slow process leading to the *trans*-chalcone. The contribution of this last species can be calculated from the difference between the initial and final spectra, indicating that about 10% of the quinoidal bases are transformed into **Ct** (Figure 7b). A reverse pH jump from the equilibrated solutions at pH 3.5 back to pH 1.0 is shown in Figure 7c. Immediately after the pH jump, the quinoidal bases are transformed into the respective flavylium cations. Calculation of the fraction of the two isomers leads to the same values of the equilibrium in Figure 3. In other words, the

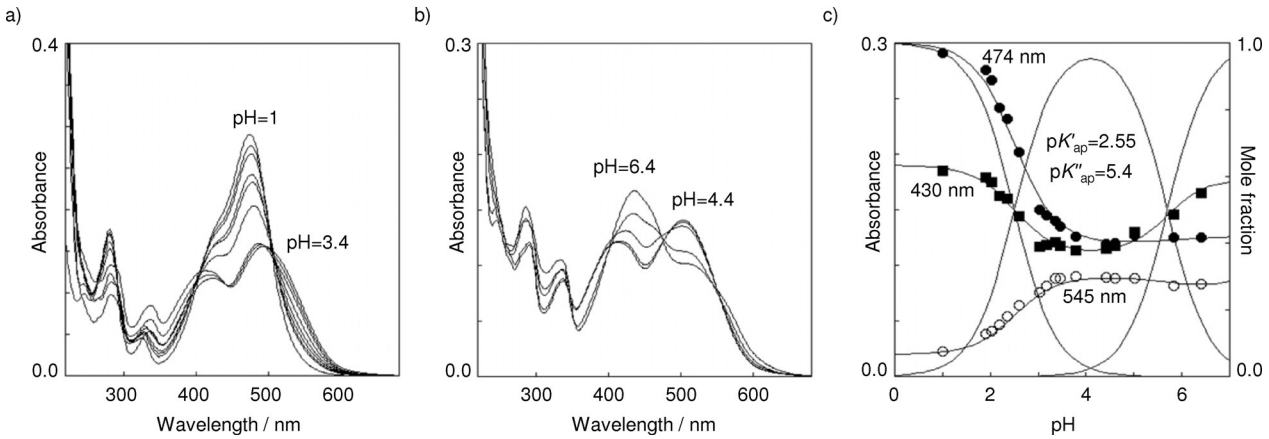

Figure 6. a) Absorption spectra corresponding to the equilibrium after a direct pH jump of the equilibrated mixture of both flavylium isomers (3.3×10^{-5} M,) in the range $1<pH<3.4$ (at pH 1.0); b) the same in the $4.4<pH<6.4$ range; c) fitting to determine the acidity constants. The values 2.55 and 5.4 can be attributed respectively to pK'_{ap} and pK''_{ap}.

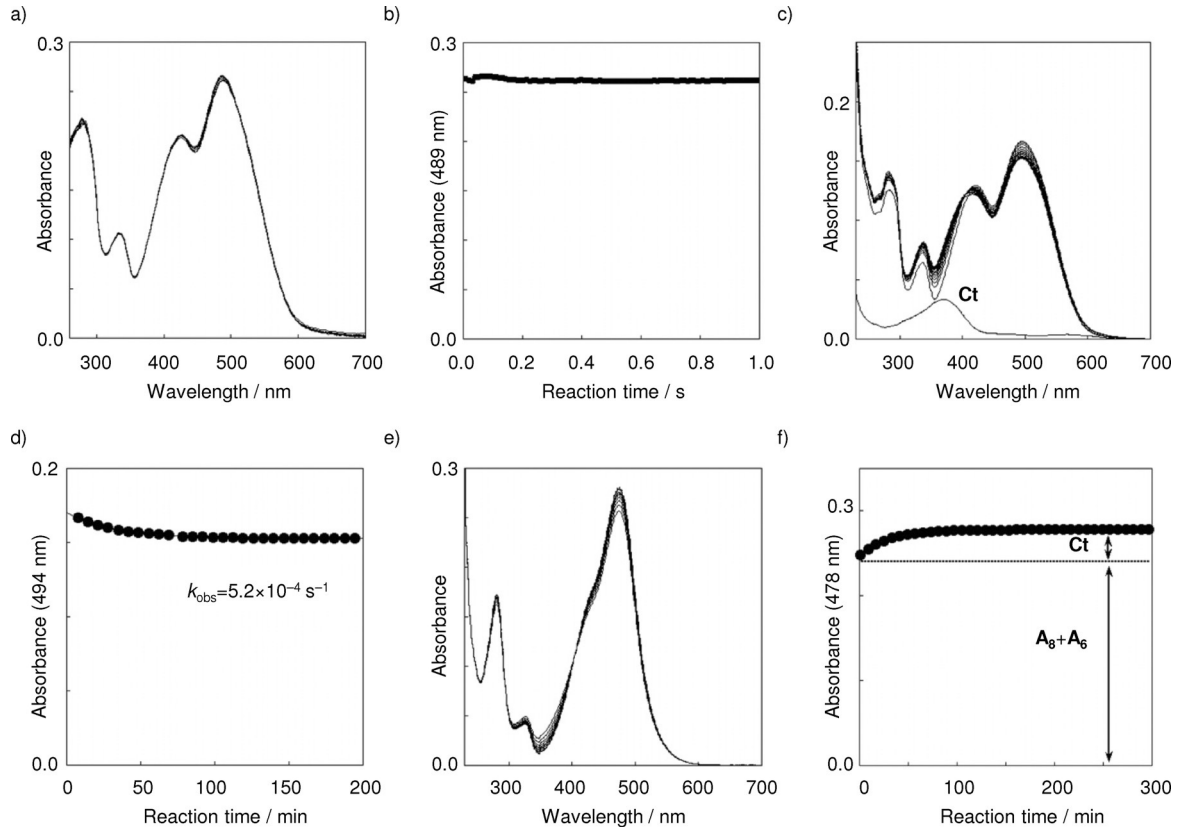

Figure 7. a) Spectral variations for a direct pH jump from equilibrated solutions of both flavylium isomers (5×10^{-5} M) at pH 1.0 to 3.4 followed by stopped flow and b) the respective kinetic trace. c) The same in a longer timescale to pH 3.5. (3.3×10^{-5} M) and d) the respective kinetic trace. e) Reverse pH jump from pH 3.5 to 1.2 and f) the respective kinetic trace. Note that subscripts denote the isomer and not oligomeric forms.

ratio of flavylium and quinoidal base isomers is 1.1 ± 0.1 between $1<pH<4$ (Figure 7c). The kinetic process observed at a longer timescale can be attributed to the conversion of the *trans*-chalcones into the respective flavylium cations. The situation is illustrated in Scheme 5.

In Figure 6a, the deprotonated species (negatively charged) are not formed. Immediately after the direct pH jump, almost equal fractions of $\mathbf{A_6}$ and $\mathbf{A_8}$ are obtained from deprotonation of the respective flavylium cations. During the first seconds after the direct pH jumps, only a very small decrease of the bases' absorbance takes place, suggesting that the fraction of hemiketals and *cis*-chalcones is very small at this stage of the kinetics. In a much longer timescale, the quinoidal bases' absorption decrease, in accordance to formation of *trans*-chal-

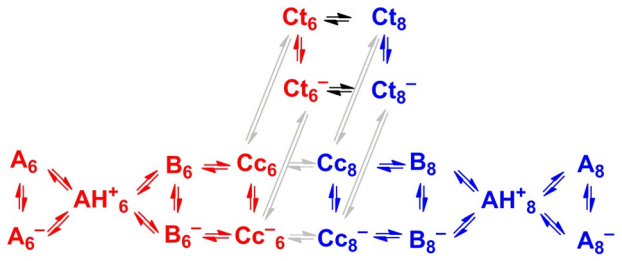

Scheme 5. Tridimensional network of chemical reactions of the system taking into account the two global acid-base equilibria [Eq. (10)] and [Eq. (12)]. Note that subscripts denote the isomer and not oligomeric forms.

cone through the slower isomerization, as reported for many flavylium derivatives, including anthocyanins. Subtracting a fraction of 0.9 of the initial spectra (of the quinoidal bases) to the last absorption spectra of Figure 6b leads to an absorption band, which can be attributed to the *trans*-chalcone. This result was corroborated by ^{1}H NMR, and is confirmed in Figure 11.

The situation at higher pH values, for the ionized species, is represented in Figure 8. The spectral variations after a pH jump to 5.9 indicate one very fast process, that is compatible to partial conversion of the quinoidal bases (mixed with the respective ionized form) into *cis*-chalcone, see below the data for the pure isomers.

A direct pH jump to 5.8, followed (after 5 min) by a reverse pH jump to 1.2 leads to the initial absorption spectra of the flavylium cation indicating that no **Ct** was formed in this timescale. On the other hand, the absorption spectra of the mixture upon a direct pH jump from the equilibrated solution at pH 1 to 5.8, after 1 week is similar to the one of the quinoidal base of the isomer **6** in equilibrium with **Ct**, see below.

In order to get more insight on the data reported in Figure 8a, stopped flow of the pure isomers was carried out (Figure 9). In both cases, the results were compatible with a decrease of the respective quinoidal base absorption to form *cis*-chalcone. In the case of isomer **6** the trace could be fitted with a biexponential function attributed to the hydration (17 s^{-1}) followed by tautomerization (0.5 s^{-1}) (Figure 8b). The trace of isomer **8** is monoexponential and can be explained by a much faster hydration (not observed by stopped flow) followed by the tautomerization (0.3 s^{-1}). A reverse pH jump back to pH 1 of the spectra obtained after 10 seconds leads to the respective pure flavylium cation isomer. This result confirms that formation of *trans*-chalcone does not take place during this timescale.

In Figure 9a, to the final spectra (10 s) of isomer **6**, a fraction of 0.81 of the initial base was subtracted, and an identical procedure was made to isomer **8** by subtracting 0.93 of the respective quinoidal base. The resulting absorption shows the formation of the two different *cis*-chalcones, exhibiting slightly

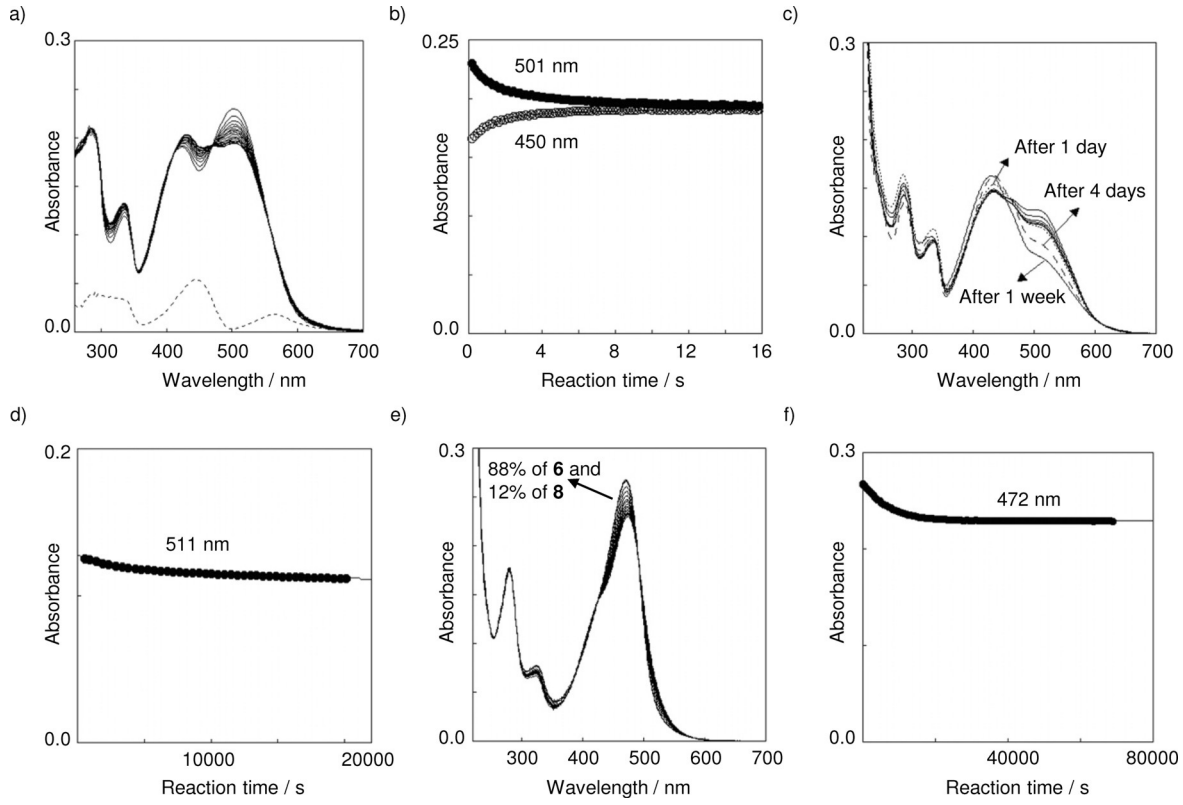

Figure 8. a) Spectral variations from a direct pH jump from equilibrated solutions of both flavylium isomers at pH 1.0 to 5.9 followed by stopped flow (5×10^{-5} M); subtraction of a fraction of 0.83 of the initial spectra gives the band represented by traced lines. b) The respective kinetic traces monitored at 501 and 450 nm. c) The same in a longer timescale to pH 5.8 (3.3×10^{-5} M) and d) respective kinetic trace monitored at 511 nm. e) Reverse pH jump from equilibrated solutions (after 1 week) pH 5.8 to 1.2 and f) the corresponding kinetic trace. Note that subscripts denote the isomer and not oligomeric forms.

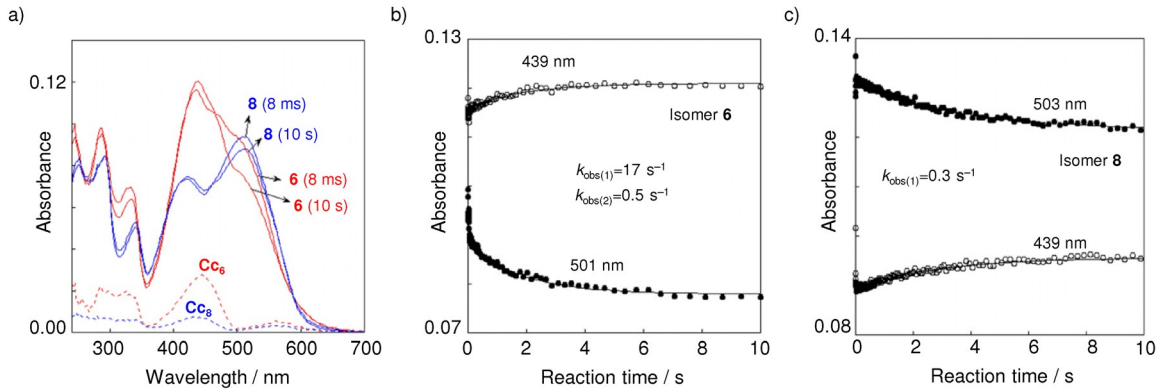

Figure 9. Stopped-flow traces upon a direct pH jump from the pure isomers (2.5×10^{-5} M) to pH 6.0: a) Absorption spectra of the pure isomers after 10 ms and at the end of this process (10 s). The process can be assigned to the formation of **Cc**; traced lines show the absorption spectra after removing a fraction of 0.81 (isomer **6**) and 0.93 (isomer **8**) of the respective quinoidal bases. **b)** Trace for the same pH jump for isomer **6**. The biexponential is attributed to the fast hydration followed by the slower tautomerization; c) same as b) but for isomer **8**. In this case, the trace is fitted with a monoexponential of the same order of magnitude observed for the ring/opening closure. Note that subscripts denote the isomer and not oligomeric forms.

shifted absorption maxima. In spite of the associate error to this mathematical procedure, this result suggests the existence of two *cis*-chalcones.

More information on the system was achieved by carrying out a sequence of direct pH jumps from solutions of each pure isomer at pH 1.0 (freshly prepared) to pH 6, letting the solution stand at pH 6.0 for 1 min and performing a reverse pH jump back to pH 1.0. As shown in Figure 10, the final spectrum is coincident with the one of the pure flavylium isomer, in both cases. These results clearly show that while evidence for the formation of a *cis*-chalcone in each isomer takes place as shown in Figure 9b and Figure 9c, the two *cis*-chalcones do not communicate at least in a timescale of few minutes.

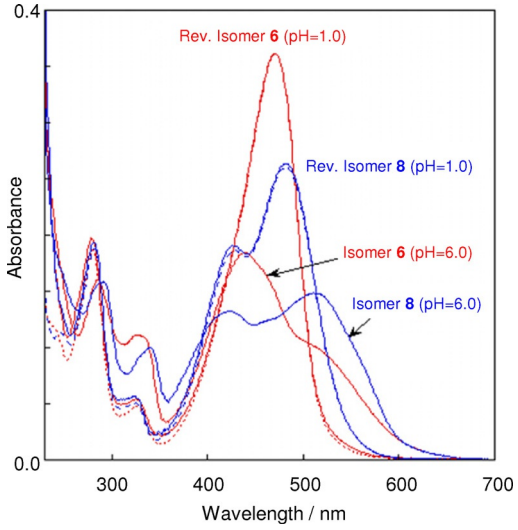

Figure 10. Absorption spectra 1 min after a direct pH jump from pure isomer (3.4×10^{-5} M) at pH 1.0 to pH 6.0 followed by a reverse pH jump back to pH 1.0. The final spectrum is coincident with the initial spectrum at pH 1.0 (traced line) before the two consecutive pH jumps, showing that no communication between the two isomers takes place in these time scales; red: isomer **6**, blue: isomer **8**.

At this point, the data presented in Figure 8a can be explained. A fraction of 0.82 of the initial mixture of the quinoidal bases was subtracted to the final spectrum, leading to the absorption spectra of the products, the traced line of Figure 8a. Inspection of this spectrum suggests the formation of a mixture of both *cis*-chalcones and a remaining absorption in the visible region compatible with quinoidal base of isomer **8**.

Considering that: 1) the two multistate isomers do not communicate (during the stopped flow), 2) formation of $\mathbf{Cc_6}$ is faster than $\mathbf{Cc_8}$, and 3) the fraction of $\mathbf{Cc_6}$ is higher than the fraction of $\mathbf{Cc_8}$, the product spectra in Figure 8a can be explained by the fact that quinoidal bases of isomer **6** are more consumed than those of isomer **8**. In other words, the initial ratio of the isomer bases (1:1) decreases the contribution of quinoidal bases of isomer **6**, because this one is more consumed than the other.

The experiment shown in Figure 10 allows to obtain the absorption spectra of the quinoidal base of both isomers. These spectra can be used to fit the final absorption at pH 4.7, as in Figure 11. Fitting was obtained for 0.45 **A** (**6**) + 0.45 **A** (**8**) + 0.1 **Ct**.

Conclusion

The two compounds studied through this work behave similarly to the parent compound apigeninidin. At lower pH values the flavylium cation is involved in a global acid-base equilibrium with the "basic" species, quinoidal base (main species), *trans*-chalcone (minor species), with hemiketal and *cis*-chalcone in neglected concentrations.

The 6,8 isomerization of flavylium cation should necessarily take place from the chalcones, the only way the two multistates have to communicate. The *cis*-chalcones of both isomers do not communicate in the timescale of minutes, but it is not possible to exclude their interconversion in longer timescales. The other alternative to explain the flavylium cation 6,8 isomerization is through the *trans*-chalcone that in principle

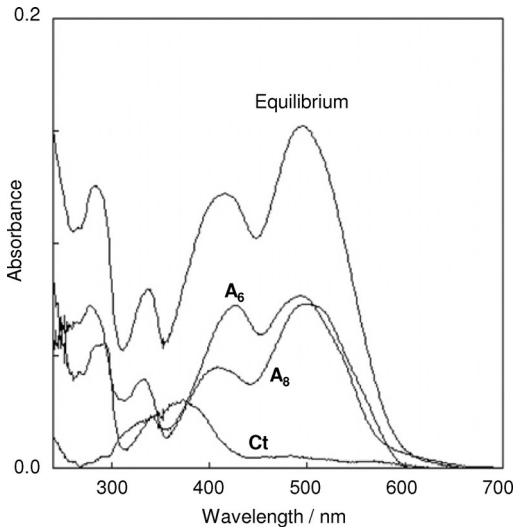

Figure 11. The absorption spectra of equilibrated solutions of the compound (3.3×10^{-5} M) at pH 3.7 can be fitted with a contribution of 0.45 **A** (**6**) + 0.45 **A** (**8**) + 0.1 **Ct**. Note that subscripts denote the isomer and not oligomeric forms.

should exhibit a fast rotation rate between the two isomers, because only one *trans*-chalcone is observed by ^{1}H NMR. At higher pH values the ionized species tend to favor the formation of the (ionized) quinoidal base of isomer **6**.

Experimental Section

Synthesis: 3-bromo-2,4,6-trihydroxybenzaldehyde (2): 2,4,6-trihydroxybenzaldehyde (**1**, 4.87 mmol) and pyridinium tribromide (1 equiv) were mixed in THF (25 mL) at −20 °C and stirred for 3 h. The reaction mixture was then quenched with water (2×100 mL), extracted with ethyl acetate (2×100 mL), washed once with brine (100 mL), and dried over anhydrous Na_2SO_4. Filtration, concentration, and silica gel column chromatography (CH_2Cl_2/CH_3OH 10:3) gave the final compound **2** as a yellow solid (89%, 1 g); ESI-MS *m/z*: 231, 233 $[M-H]^-$.

6-, 8-Bromo-apegininidin (6, 8): 3-bromo-2,4,6-trihydroxybenzaldehyde (**2**, 0.86 mmol) and 4-hydroxyacetophenone (**3**, 1.03 mmol) were dissolved in HOAc (10 mL), and anhydrous HCl (g) was bubbled through the solution for 60 min. The reaction was stirred at rt for 24 h. Water (10 mL) was added to the mixture, and the product was extracted with diethyl ether (3×10 mL). The aqueous phase was concentrated and prepurified by elution through C18 silica gel. The residue was redissolved in MeOH/H_2O 85:15 (1% HCOOH), and the purification of products **6** and **8** was performed by semipreparative HPLC. The semipreparative HPLC system (Merck Hitachi, Darmstadt, Germany) was composed by an L-7100 quaternary pump, a L-7200 autosampler injector with loop of 500 μL, an L-7360 column oven, and an L-7420 UV/Vis detector. The stationary phase was composed by a reversed-phase C18 column (Merck, Darmstadt, Germany; 250 mm×4.6 mm i.d., 5 μm pore size) thermostatted at 25 °C, and the eluents were A) water/formic acid 9:1 (*v*:*v*) and B) CH_3CN, with the following gradient: 10–35% B over 50 min at a flow rate of 1 mL min^{-1}. Detection wavelength was set to 475 nm. After concentration, the puritiy of the compounds was checked by HPLC with diode-array detection (DAD). After lyophilization, the isomers were obtained as an orange solid (6%, 20 mg). The full structural characterization was achieved by LC-DAD/ESI-MS and NMR analysis.

^{1}H NMR (600.13 MHz, CD_3OD/CF_3COOH 90:10): *Isomer* ***6****:* $\delta=9.16$ (d, 8.8 Hz, 1H, 4**C**), 8.33 (d, 8.9 Hz, 2H, 2′**B**, 6′**B**), 8.12 (d, 8.8 Hz, 1H, 3**C**), 7.13 (s, 1H, 8**A**), 7.08 ppm (d, 8.9 Hz, 2H, 3′**B**, 5′**B**); *Isomer* ***8****:* $\delta=9.08$ (d, 8.7 Hz, 1H, 4**C**), 8.39 (d, 8.9 Hz, 2H, 2′**B**, 6′**B**), 8.10 (d, 8.7 Hz, 1H, 3**C**), 7.10 (d, 8.9 Hz, 2H, 3′**B**, 5′**B**), 6.85 ppm (s, 1H, 6**A**).

^{13}C NMR (125.77 MHz, CD_3OD/CF_3COOH 90:10): *Isomer* ***6****:* $\delta=171.6$ (2**C**), 166.5 (4′**B**), 165.6 (7**A**), 156.8 (8**aA**), 155.2 (5**A**), 147.9 (4**C**), 132.0 (2′**B**, 6′**B**), 119.7 (1′**B**), 117.0 (3′**B**, 5′**B**), 111.9 (4**aA**), 109.3 (3**C**), 99.2 (6**A**), 94.7 ppm (8**A**); *Isomer* ***8****:* $\delta=171.6$ (2**C**), 167.2 (7**A**), 166.5 (4′**B**), 158.1 (5**A**), 154.4 (8**aA**), 147.9 (4**C**), 132.0 (2′**B**, 6′**B**), 119.7 (1′**B**), 117.0 (3′**B**, 5′**B**), 113.0 (4**aA**), 109.3 (3**C**), 101.3 (6**A**), 87.9 ppm (8**A**); LC-DAD/ESI-MS *m/z* 333, 335 $[M]^+$.

HPLC: HPLC analyses were performed on a Merck-Hitachi L-7100 apparatus with a 250×4.6 mm i.d. reversed-phase ODS C18 column at 25 °C; detection was carried out using an L-7450A diode array detector (DAD). The eluents were A) H_2O/HCOOH (9:1) and B) CH_3CN. The gradient consisted of 10–35% B for 50 min at a flow rate of 1 mL min^{-1}. The column was washed with 100% B for 10 min and then stabilized with the initial conditions for another 10 min. The semipreparative HPLC system (Knauer WellChrom, Berlin, Germany) was composed of a solvent organizer K-1500, a K-1001 quaternary pump, a manual injector with loop of 750 μL, and an S3210 UV/Vis detector. The stationary phase was composed of a reversed-phase C18 column (Merck, Darmstadt, Germany, 250 mm×4.6 mm i.d.) and the eluents were A) water/formic acid 9:1 (*v*:*v*) and B) CH_3CN, with the following gradient: 0–35% B over 50 min at a flow rate of 1 mL min^{-1}. Detection wavelength was set to 330 nm.

To study the evolution of the isomers with pH variation, 20% EtOH (aq) solutions ($C=0.27$ mM) were prepared at three different pH levels (1, 4, and 6), which were followed over time by HPLC. Area intensities of chromatographic peaks were taken at the maximum absorption wavelength of each isomer (**6**, λ_{max} 478 nm; **8**, $\lambda_{max}=$ 496 nm).

LC-DAD/ESI-MS: LC-DAD/ESI/MS analyses were performed on a Finnigan Surveyor series liquid chromatograph equipped with a Finnigan LCQ mass detector (Finnigan Corp., San Jose, CA, USA) and an atmospheric-pressure ionization (API) source using an ESI interface. The samples were analyzed on a reversed-phase column (150×4.6 mm, 5 μm, C18) at 25 °C using the same eluents, gradients, and flow rates used for HPLC analysis. The capillary voltage was 4 V, and the capillary temperature 275 °C. Spectra were recorded in positive- and negative-ion modes between *m/z* 120 and 1500. The mass spectrometer was programmed to do a series of three scans: a full mass (MS), a zoom scan of the most intense ion in the first scan (MS^2), and an MS–MS of the most intense ion using relative collision energy of 30 and 60 V (MS^3).

NMR: ^{1}H NMR (600.13 MHz) and ^{13}C NMR (125.77 MHz) spectra were recorded in CD_3OD/CF_3COOH (90:10) on a Bruker-Avance 600 spectrometer (Billerica, MA, USA) at 303 K and with tetramethylsilane (TMS) as an internal standard (chemical shifts, δ in ppm; coupling constants, *J*, in Hz). ^{1}H chemical shifts were assigned using 2D NMR (correlation spectroscopy, COSY) experiments, while ^{13}C resonances were assigned using 2D NMR techniques: heteronuclear multiple-bond correlation spectroscopy (gHMBC) and heteronuclear single quantum coherence spectroscopy (gHSQC). The delay for the long-range C/H coupling constant was optimized to 7 Hz.

UV/Vis spectroscopy: The pH of the solutions was adjusted by addition of HCl, NaOH, or Theorell and Stenhagen's universal buffer,[15] and pH was measured in a Radiometer Copenhagen PHM240 pH/ion meter (Brønshøj, Denmark). UV/Vis absorption spectra were recorded in a Varian-Cary 100 Bio or 5000 spectrophotometer (Palo Alto, CA, USA). Direct pH jumps were carried out by addition of the necessary amount of base and buffer (typically 2 mL) to get the desired final pH, from a previous equilibrated solution of flavylium cations at pH 1.0 (1 mL). This way, the stock solution of the compound was diluted by a factor of 3 upon a direct pH jump. The reverse pH values were performed from equilibrated solutions at moderately acidic pH values back to very acidic pHs. The spectra of pure isomers were taken using similar techniques immediately after dissolving of the pure compound. To avoid significant isomerization during the solubilization process, the required volume of acid was first added (as the isomerization is slower at acidic conditions) followed by the required volume of EtOH/water 1:4 mixture. All the fitting procedures were carried out using the program solver from Microsoft Excel.

Stopped flow experiments: These were conducted in an Applied Photophysics SX20 stopped-flow spectrometer (Leatherhead, UK) provided with a PDA.1/UV photodiode-array detector with a minimum scan time of 0.65 ms and a wavelength range of 200 nm to 735 nm. For direct pH jumps, stock solutions of the compound at pH 1 were placed in one syringe, and the necessary amount of base and buffer to obtain the desired final pH in another syringe. Upon mixing, the concentration of the compound was diluted by a factor of 2. Similarly, reverse pH jumps were carried out by placing an equilibrated solution of the compound at a given pH in one syringe and the respective amount of HCl in the second syringe to obtain the desired final pH values. A small volume of sample was recovered after mixing to confirm the pH.

Acknowledgements

The authors thank Dr. Zélia Azevedo (Faculty of Sciences, University of Porto) for the MS analysis and Dr. Mariana Andrade (Center of Materials, University of Porto) for the NMR analysis. Luís Cruz and Nuno Basilio gratefully acknowledge the postdoctorate grants from the Fundação para a Ciência e a Tecnologia (FCT) (SFRH/BPD/72652/2010 and SFRH/BPD/84805/2012, respectively). The authors also thank the financial support of national funds from the FCT and Fundo Europeu de Desenvolvimento Regional (FEDER) under Program PT2020 (project 007265-UID/QUI/50006/2013).

Keywords: 6,8 flavylium rearrangement · 6-bromo-apigeninidin · 8-bromo-apigeninidin · anthocyanins · UV/Vis

[1] J. M. Awika, L. W. Rooney, R. D. Waniska, *J. Agric. Food Chem.* **2004**, *52*, 4388 – 4394.
[2] J. M. Baranac, D. S. Amic, *J. Agric. Food Chem.* **1990**, *38*, 2111 – 2115.
[3] B. Busetta, J. C. Colleter, M. Gadret, *Acta Crystallogr. Sect. B* **1974**, *30*, 1448 – 1451.
[4] B. Geera, L. O. Ojwang, J. M. Awika, *J. Food Sci.* **2012**, *77*, C566 – C572.
[5] T. Mas, *Synthesis* **2003**, 1878 – 1880.
[6] J. G. Sweeny, G. A. Iacobucci, *Tetrahedron* **1981**, *37*, 1481 – 1483.
[7] J. G. Sweeny, G. A. Iacobucci, *J. Agric. Food Chem.* **1983**, *31*, 531 – 533.
[8] R. Brouillard, G. A. Iacobucci, J. G. Sweeny, *J. Am. Chem. Soc.* **1982**, *104*, 7585 – 7590.
[9] F. Pina, M. J. Melo, C. A. T. Laia, A. J. Parola, J. C. Lima, *Chem. Soc. Rev.* **2012**, *41*, 869 – 908.
[10] R. Brouillard, J. E. Dubois, *J. Am. Chem. Soc.* **1977**, *99*, 1359 – 1364.
[11] F. Pina, J. Oliveira, V. de Freitas, *Tetrahedron* **2015**, *71*, 3107 – 3114.
[12] Ø. Bjorøy, S. Rayyan, T. Fossen, Ø. M. Andersen, *J. Agric. Food Chem.* **2009**, *57*, 6668 – 6677.
[13] L. Jurd, *J. Org. Chem.* **1963**, *28*, 987 – 991.
[14] H. HyperChem(TM) Professional 7.51, Inc., 1115 NW 4th Street, Gainesville, Florida 32601, USA.
[15] W. F. Küster, A. Thiel, *Tabelle per le Analisi Chimiche e Chimico-fisiche, 12th ed.*, Hoepli, Milano, **1982**, pp. 157 – 160.

Received: November 18, 2015
Revised: January 22, 2016
Published online on February 25, 2016

